Passive Seismic Characterization of High Priority Salt Jugs, Barton Well Field, Hutchinson, Kansas

Shelby Peterie, Julian Ivanov, Richard Miller, Amanda Livers,
Brett Bennett, Bryan Brooks, Joey Fontana, Brett Judy,
Sarah Morton, Ryan Nelson, Jordan Nolan,
Brett Wedel, and Yao Wang

Kansas Geological Survey
1930 Constant Avenue
Lawrence, KS 66047

Final Report to

Ed Lindgren
Burns & McDonnell Engineering Company
9400 Ward Parkway
Kansas City, MO 64114
(816) 822-3138

Open-file Report 2015-28 April 2, 2015

The Kansas Geological Survey makes no warranty or representation, either express or implied, with regard to the data, documentation, or interpretations or decisions based on the use of this data including the quality, performance, merchantability, or fitness for a particular purpose. Under no circumstances shall the Kansas Geological Survey be liable for damages of any kind, including direct, indirect, special, incidental, punitive, or consequential damages in connection with or arising out of the existence, furnishing, failure to furnish, or use of or inability to use any of the database or documentation whether as a result of contract, negligence, strict liability, or otherwise. This study was conducted in complete compliance with ASTM Guide D7128-05. All data, interpretations, and opinions expressed or implied in this report and associated study are reasonably accurate and in accordance with generally accepted scientific standards.

Preliminary Passive Seismic Characterization of High Priority Salt Jugs, Barton Well Field, Hutchinson, Kansas

Executive Summary

This applied research project correlated measured shear-wave velocities with the condition of rock above dissolution voids, targeting the stress as related to shear wave velocity of the overburden. Shear-wave velocities were estimated using passive surface wave data acquired along a total of five profiles that intersected 7 wells. Multi-channel analysis of surface waves (MASW) was used to estimate the shear-wave velocity, loosely map stratigraphic contacts above the top of the "three finger" dolomite, and evaluate the relative strength of the rock above the wells. If necessary, a recommendation for additional investigation where voids are suspected to have the potential for vertical migration will be made.

Passive MASW profiles were acquired during two surveys at the Barton Well Field in Hutchinson, Kansas, on October 15, 2014, and January 22, 2015. Five lines and a surface 2-D grid of receivers were positioned over key wells during the initial investigation. During the follow-up survey, two lines and the 2-D surface grid of receivers were deployed for an additional, focused investigation of two lines from the first survey to enhance the interpretation at wells 20, 21, and 33. Surface waves with frequencies as low as 3 hertz (Hz) were recorded with an average depth of investigation 40-60 meters (m), and in some places exceeding 60 m, successfully sampling deep within bedrock.

With shear-wave velocity being a function of shear modulus and density (the shear modulus is the ratio of stress over strain), it is possible to quantify relative stress of overburden rocks (shear modulus) by shear velocity values. Local increases in shear velocity without changes in lithology can be equated to increased stress associated with overburden roof load over dissolution jugs. Relative shear velocity lows may be associated with collapse features whose vertical movement has been arrested by bulking, reduced stress to within roof rock strength, or changes in strength due to geologic features related to natural variation in deposition or erosion.

Shear velocities within most of the study area are indicative of a normal stress regime and natural geologic variation. Elevated shear velocity in the shale overburden above well 33 relative to other lines at this site suggests elevated stress and possible risk of roof failure and vertical migration of the void. However, a priori information from a past sonar survey indicates a relatively small void at this location. While the magnitude of the velocity anomaly is indicative of elevated stress and potential failure, the relatively small volume of this jug will severely limit the amount of collapse breccia from roof rocks that can collect in this relatively small void thereby minimizing any future vertical migration of the void to depths well below ground surface.

Introduction

Material properties (specifically strength and stress accumulations) measured as a function of depth above abandoned salt jugs in Hutchinson, Kansas, appear to be related to the mobility and upward migration potential of these jugs. Localized increases in stress (as indicated by increased shear-wave velocity) above subterranean voids is one indicator of an increased potential for roof failure and void migration (Eberhart-Phillips et al., 1989; Dvorkin et al., 1996; Khaksar et al., 1999; Sayers, 2004). Previous studies, using both active and passive seismic wavefield characteristics, suggest that perturbations in the shear-wave velocity field immediately above voids can be correlated to characteristics of the unsupported roof spans of salt jugs in the Hutchinson area (Sloan et al., 2010).

The strength of individual rock layers can be qualitatively described in terms of stiffness/rigidity and empirically estimated from relative comparisons of shear-wave velocity measurements. Shear-wave velocity is directly proportional to stress and inversely related to non-elastic strain. Since the shear-wave velocity of earth materials changes when stress and any associated elastic strain on those materials becomes "large," it is reasonable to suggest load-bearing roof rock above mines or dissolution voids may experience elevated shear-wave velocities due to loading between pillars or, in the case of voids, loading between supporting side walls. This localized increase in shear velocity is not related to increased strength, but increased load as defined by Young's Modulus. High-velocity shear-wave "halos" encompassing low-velocity anomalies are suggested to be key indicators of near-term roof failure. All these phenomena have been observed within the overburden above voids in the Hutchinson Salt Member in Hutchinson at depths greater than 30 m below the bedrock surface.

Previous active seismic reflection experiments in Hutchinson have detected areas with elevated shear-wave velocity likely indicative of an imminent risk for vertical migration of specific salt jugs (Sloan et al., 2010). The lack of necessary ultra low-frequency surface waves in the recorded wavefield have negated attempts to use active source multi-channel analysis of surface waves (MASW) to estimate shear velocity in the lithified rocks near the top of bedrock (Miller et al., 2009). Uncontrolled, local industrial and transportation activities represent sound sources that have produced the necessary low frequencies and, when recorded and processed using passive methods, have extended the imaging depth to over 60 m (Miller, 2011).

Passive surface-wave recording allows random sources of seismic energy (trains, manufacturing facilities, heavy vehicles on roadways, processing plants, heavy construction equipment, etc.), considered noise on active surveys, to be recorded so that data processing enhancements and specialized processing methods can be used to calculate the 1-D shear wave velocity function. The key to this method is the ability to estimate shear-wave velocities to depths double or more than otherwise possible with standard active sources at a particular site (Park et al., 2004). Passive MASW experiments have previously been used in Hutchinson to effectively identify void roofs with elevated stress and an elevated risk of vertical migration (Ivanov et al., 2013).

Geologic and Geophysical Setting

The Permian Hutchinson Salt Member occurs in central Kansas, northwestern Oklahoma, and the northeastern portion of the Texas Panhandle, and is prone to and has an extensive history of dissolution and formation of sinkholes (Figure 1). In Kansas, the Hutchinson Salt Member possesses an average net thickness of 75 m and reaches a maximum of over 150 m in the

southern part of the basin. Deposition occurring during fluctuating sea levels caused numerous halite beds, 0.2 to 3 m thick, to be formed interbedded with shale, minor anhydrite, and dolomite/magnesite. Individual salt beds may be continuous for only a few miles despite the remarkable lateral continuity of the salt as a whole (Walters, 1978).

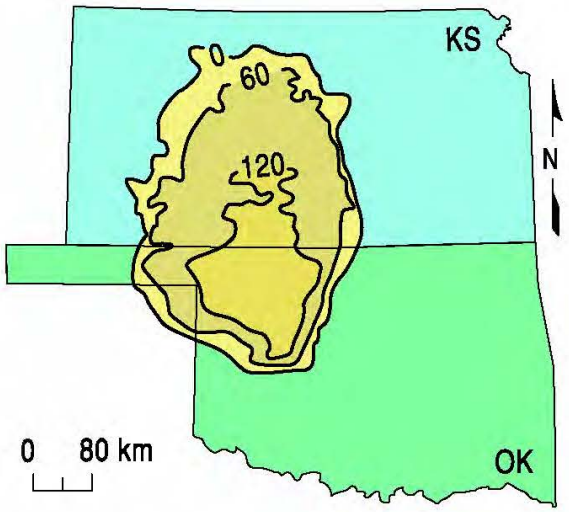

Figure 1. Approximate extent of salt formation, with contour intervals expressed in meters.

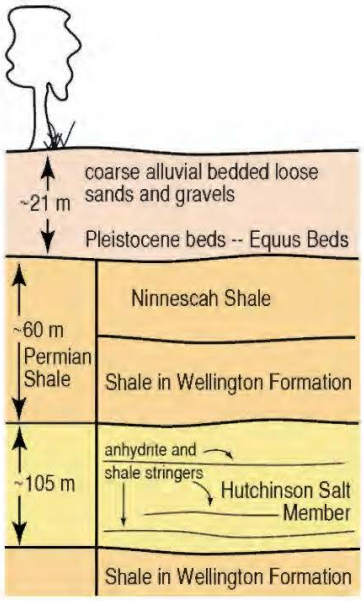

Figure 2. Generalized geology.

The distribution and stratigraphy of the salt is well documented (Dellwig, 1963; Holdoway, 1978; Kulstad, 1959; Merriam, 1963). The salt reaches a maximum thickness in central Oklahoma and thins to depositional edges on the north and west, an erosional subcrop on the east, and facies changes on the south. The increasing thickness toward the center of the salt basin is due to a combination of increased salt and more and thicker interbedded anhydrites. The Stone Corral Formation (a well documented seismic marker bed) overlies the salt throughout Kansas (McGuire and Miller, 1989). Directly above the salt at this site is a thick sequence of Permian shales.

The upper 760 m of rock at this site is Permian shale (Merriam, 1963). The Chase Group (top at 300 m deep), lower Wellington Shale (top at 245 m deep), Hutchinson Salt (top at 120 m deep), upper Wellington Shales (top at 75 m deep), and Ninnescah Shale (top at 25 m deep) make up the packets of reflecting events easily identifiable and segregated within the Permian portion of the section (Figure 2). Bedrock is defined as the top of the Ninnescah Shale with the unconsolidated Pliocene-Pleistocene Equus beds making up the majority of the upper 30 m of sediment. The thickness of Quaternary alluvium that fills the stream valleys and paleosubsidence features goes from 0 to as much as 90 m, depending on the dimensions of the features.

Recent dissolution of the salt and resulting subsidence of overlying sediments forming sinkholes has generally been associated with mining or saltwater disposal (Walters, 1978). Historically, these sinkholes can manifest themselves as a risk to surface infrastructure. The rate of surface subsidence can range from gradual to very rapid. Besides risks to surface structures, subsidence features potentially jeopardize the natural segregation of ground-water aquifers,

greatly increasing their potential to negatively impact the environment (Whittemore, 1989, 1990). Natural sinkholes resulting from dissolution of the salt by localized leaching within natural flow systems which have been altered by structural features (such as faults and fractures) are not uncommon west of the main dissolution edge (Merriam and Mann, 1957).

Caprock and its characteristics are a very important component of any discussion concerning dissolution, subsidence, and formation of sinkholes. The Permian shales (Wellington and Ninnescah) that overlay the Hutchinson Salt Member are about 60 m thick in this area and are characterized as generally unstable when exposed to freshwater, being susceptible to sloughing and collapse (Swineford, 1955). These Permian shales tend to be red or reddish-brown and are commonly referred to as "red beds." Permian red beds are extremely impermeable to water and have provided an excellent seal between the freshwaters of the Equus beds and the extremely water-soluble Hutchinson Salt Member. The modern-day extent of the Hutchinson Salt is due to the protection from freshwater provided by these red beds.

Isolating the basal contact of the Wellington Formation provides key insights into the general strength of roof rock expected if dissolution-mined salt jugs (salt jugs are the cavities or voids, often shaped like jugs, in the salt that forms after salt has been solution mined in proximity to the wells) reach the top of the salt zone. Directly above the salt/shale contact is an approximately 6 m thick dark-colored shale with joint and bedding cracks filled with red halite (Walters, 1978). Once unsaturated brine comes in contact with this shale layer, these red-halite-filled joints and bedding planes are rapidly leached, leaving an extremely structurally weak layer.

Study I: Initial Investigation, October 2014

Field Layout and Data Acquisition

To ensure the highest quality data, receivers were deployed during the day and train data were recorded at night when cultural and industrial noise was minimal to provide optimum signal-to-noise. Analysis of the previous seismic energy sources captured during passive recording at a similar site in Hutchinson clearly indicated trains from a distance of 3 kilometers (km) or more away provided the best broad spectrum, low-frequency seismic energy (Miller, 2011). Because seismic energy with characteristics best suited for the purpose of this study may arrive when trains are at a distance greater than can be detected by spotters, seismic records were recorded continuously during acquisition to ensure that optimum data was recorded.

Data were acquired on the night of October 15, 2014. Five seismic lines were oriented over seven wells with known locations (33, 57, 32, 28, 26, 21, and 20) and a 2D grid was set out to determine the direction of passive seismic energy (Figure 3). Seismic receivers were single GeoSpace GS11D 4.5 Hz geophones spaced at 3 m intervals. The seismic lines varied in length (Table 1) and totaled nearly 1 km. Slight bends were required in lines 1, 2, and 3 to avoid existing obstacles (e.g. houses). The 2-D monitoring grid consisted of 144 receivers spaced at 5 m and configured to form four concentric expanding squares with 10, 30, 50, and 70 m sides. Data were recorded during one night with a 500+ channel 24-bit Geometrics Geode distributed seismic system. Seismic records were 30 seconds (s) long with a 2 millisecond (ms) sampling interval. In total, 756 seismic records equivalent to 22.7 gigabytes (Gb) of data were recorded.

Figure 3. Aerial photo with GPS locations of seismic lines from the initial survey in October 2014 (yellow lines) and follow-up survey in January 2015 (red lines) and locations of wells (white circles) in the study area.

Table 1. Number of receivers, total lengths, and wells located within each seismic line acquired in the initial investigation.

	# of receivers	line length (m)	well(s)
line 1	52	153	33
line 2	51	150	57
line 3	53	156	32
line 4	96	285	26, 28
line 5	72	213	21, 20

Processing and Analysis

Data were processed using algorithms developed at the KGS. The passive method used for this study is well established and provided good quality results at a similar site in Hutchinson (Park et al., 2004; Ivanov et al., 2013). Continuous acquisition records energy from energy sources at various orientations with respect to the seismic line. The 2-D grid was deployed to evaluate and optimize source alignment with respect to each 1-D seismic line to effectively identify void roofs with elevated stress and therefore an elevated risk of vertical migration.

For each line, the surface wave amplitudes recorded by the 2-D grid were plotted as phase velocity versus frequency for a range of azimuths from 0 to 360 degrees with respect to the seismic line to determine which record had the best broad band, low frequency source with an azimuth near parallel to the line (Figure 4). The seismogram with optimum source characteristics was selected and divided into the shortest groups of receivers ("spread length") determined to provide dispersion patterns on phase velocity versus frequency plots with high amplitude fundamental mode Rayleigh wave energy and minimal higher-order surface wave interference (Figure 5). Fundamental mode dispersion curves were picked and inverted to obtain a 2-D section of shear wave velocity (V_S) as a function of depth. The apparent velocity (v_{app}) is:

$$v_{app} = \frac{v_{act}}{(\cos\theta)} \tag{1}$$

where v_{act} is the actual seismic velocity and θ is the azimuth of the source with respect to the seismic line determined from the azimuth versus frequency plot. Thus, the increase in velocity (Δv) is:

$$\Delta v = \frac{1}{\cos\theta} - 1 \tag{2}$$

Equation 2 was used to calculate the increase in velocity due to the source azimuth for each line (Table 2).

Table 2. Directions of the passive seismic sources and the seismic lines (in degrees counterclockwise from east), the angle of the source with respect to the line (θ), and the percent increase in apparent velocity (Δv) attributable to oblique source orientations.

	source orientation	line orientation	θ	Δv
line 1	160°	170°	10°	1.5%
line 2	30°	30°	0°	0%
line 3	35°	20°	15°	3.5%
line 4	60°	45°	15°	3.5%
line 5	85°	90°	5°	< 1%

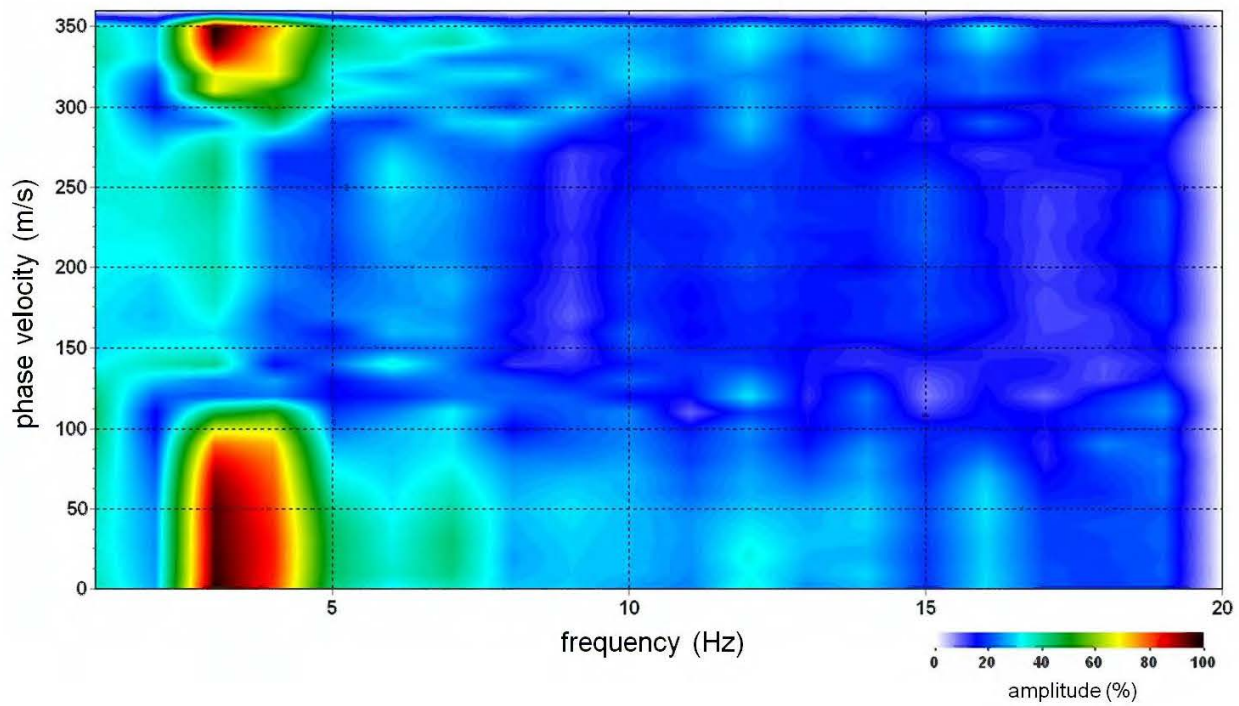

Figure 4. Azimuth plot indicating the direction of the dominant passive source energy (in degrees counter-clockwise from east). Here, the dominant passive source energy is centered on 30°.

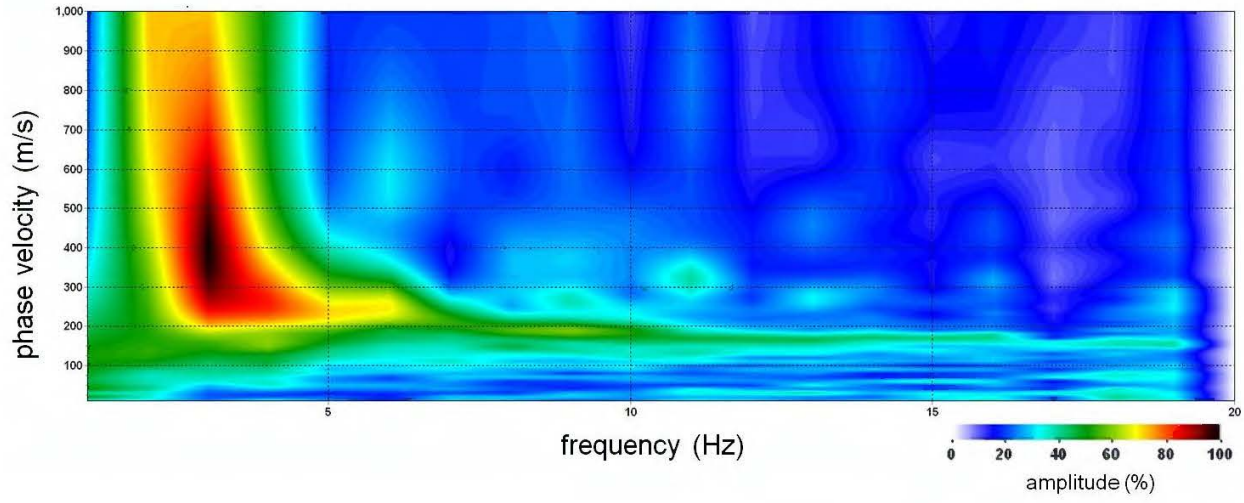

Figure 5. Representative dispersion pattern with high signal-to-noise ratio of the fundamental mode Rayleigh wave.

Results and Interpretation

Line 1 is oriented NW-SE and is centered on well 33. The velocity of the upper layer is approximately 200 meters per second (m/s) (Figure 6), consistent with the shear-wave velocity of unconsolidated sediment. At 20-30 m depth, the average velocity is approximately 350 m/s, which is indicative of the top of bedrock. Shale bedrock velocities exceed 400 m/s, suggesting a possible increase in load. The shear-wave velocity of bedrock and depth of surface wave penetration are greater on this line relative to the other lines at this site, which may suggest elevated stress. Additional data is required at well 33 to fill in and improve the dataset and enhance the interpretation.

Line 2 is oriented SW-NE and is centered on well 57. The velocity of the upper 20-30 m is 150-300 m/s (Figure 7), consistent with shear-wave velocities expected for unconsolidated sediment. Beneath 20-30 m the velocity exceeds 300 m/s, indicative of shale bedrock. Bedrock velocity is slightly greater at the SW end of the line, consistent with the observations for line 1. The dispersion pattern of the fundamental mode Rayleigh wave energy is high resolution on the phase velocity versus frequency plots, with minimal interference of higher modes energy or other sources of noise. The resulting 2-D Vs profile is high-confidence and is suggestive of a normal stress regime from the surface to 40 m depth.

Line 3 is oriented SW-NE and is centered on well 32. The average velocity of the upper 20-30 m is approximately 200 m/s (Figure 8), consistent with the shear-wave velocity of unconsolidated sediment. Beneath 20-30 m the velocity exceeds 300 m/s, indicative of shale bedrock. The velocity gradient at the top of bedrock is relatively gentle, suggesting weathering. The dispersion pattern of the fundamental mode Rayleigh wave energy is high resolution on the phase velocity versus frequency plots, with minimal interference. The resulting 2-D Vs profile is high confidence and is suggestive of a normal stress regime from the surface to 60 m depth.

Line 4 is oriented SW-NE and extends over wells 26 and 28. The average velocity of the upper 30 m ranges from 150-275 m/s (Figure 9), consistent with the shear-wave velocity of unconsolidated sediment. The top of bedrock is at a depth of approximately 30 m with velocity exceeding 300 m/s. The majority of the profile is representative of a normal stress regime. There is a slight increase in velocity at approximately 50 m depth near well 26 at the northeast end of the line. However, dispersion patterns on the northeast end of line 4 have lower signal-to-noise ratio of the fundamental mode Rayleigh wave and thus greater uncertainty. Although the velocity increase near well 26 may suggest a relatively small increase in stress, confidence in this velocity anomaly is low to moderate.

Line 5 is oriented N-S and extends over wells 20 and 21. Line 5 required a larger processing spread length for sufficient resolution of the fundamental mode Rayleigh wave on phrase velocity versus frequency plots. Therefore, the 2-D Vs profile covers a smaller area than the receiver line was initially designed to investigate. The profile spans well 21, but does not extend directly over well 20. The average velocity of the upper 20 m is approximately 200 m/s (Figure 10), consistent with the shear-wave velocity of unconsolidated sediment. Beneath 20 m the velocity exceeds 325 m/s, indicative of shale bedrock. Although the resulting 2-D Vs profile is suggestive of a normal stress regime, confidence is low due to the low signal-to-noise ratio of the fundamental mode Rayleigh wave. The larger spread length used for processing requires acquisition with a longer seismic line to extend the investigation area over the wells and increase confidence in the interpretation.

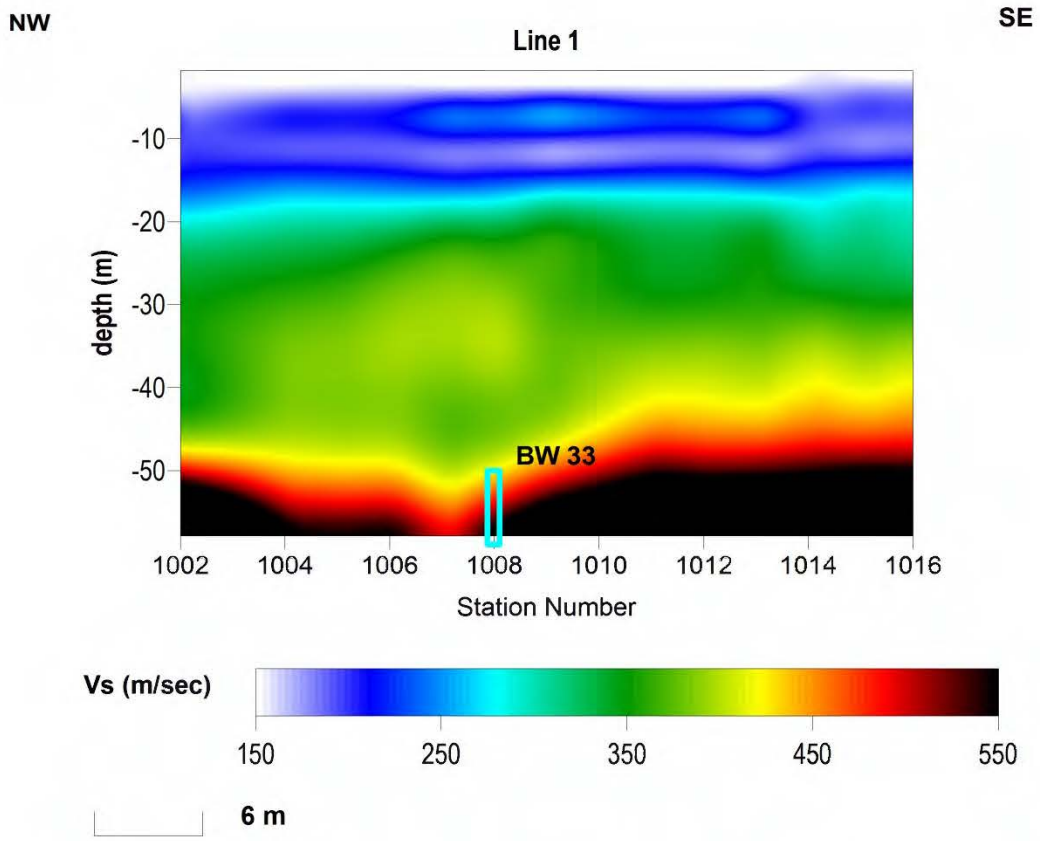

Figure 6. Final shear-wave velocity profile from line 1 of the initial survey. Approximate well location is indicated at the bottom of the profile.

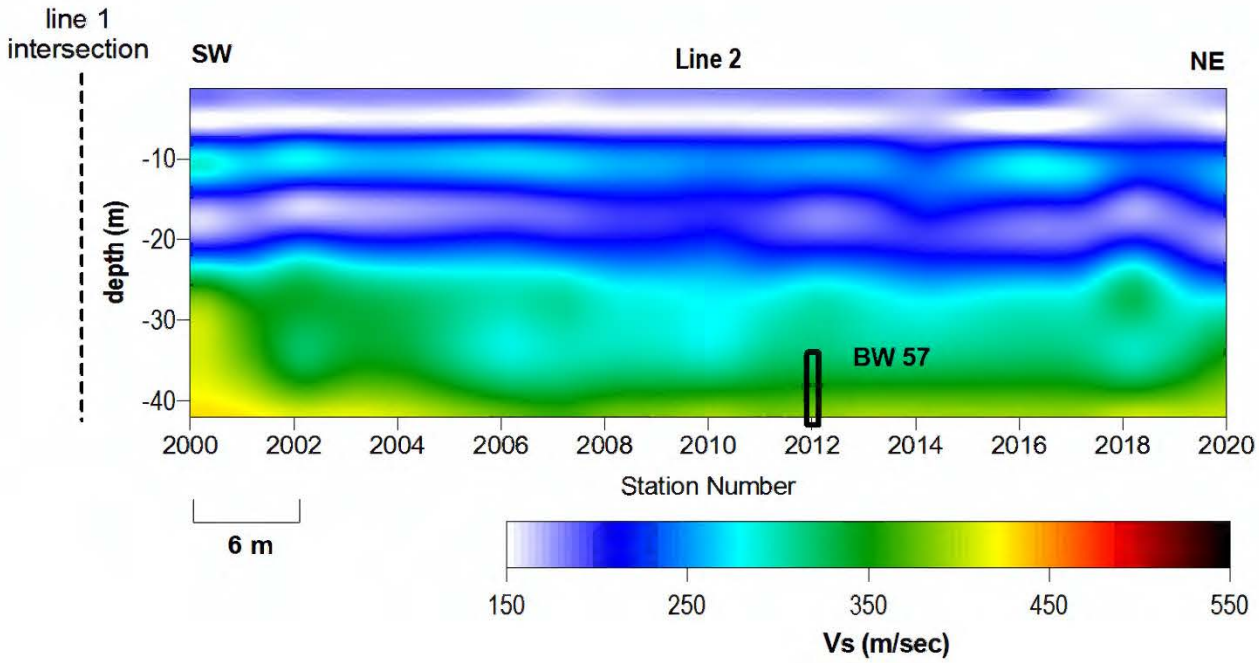

Figure 7. Final shear-wave velocity profile from line 2 of the initial survey. Approximate well location is indicated at the bottom of the profile. The dashed black line represents the line 1 intersection.

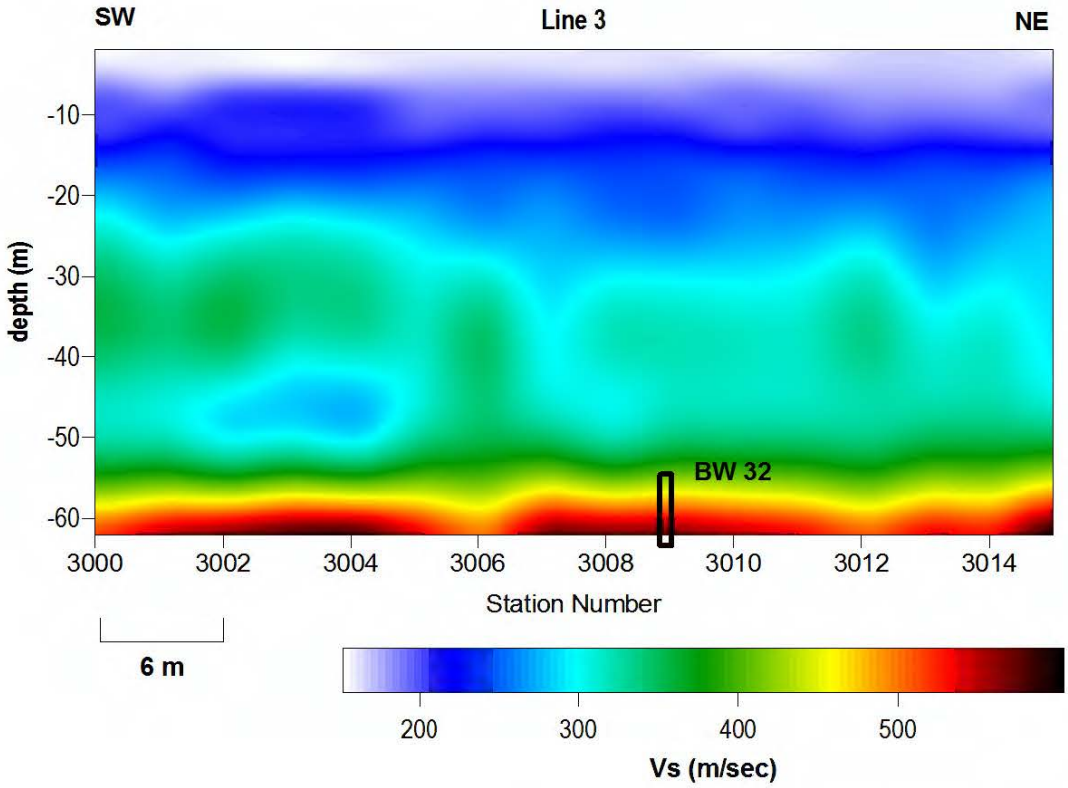

Figure 8. Final shear-wave velocity profile from line 3 of the initial survey. Approximate well location is indicated at the bottom of the profile.

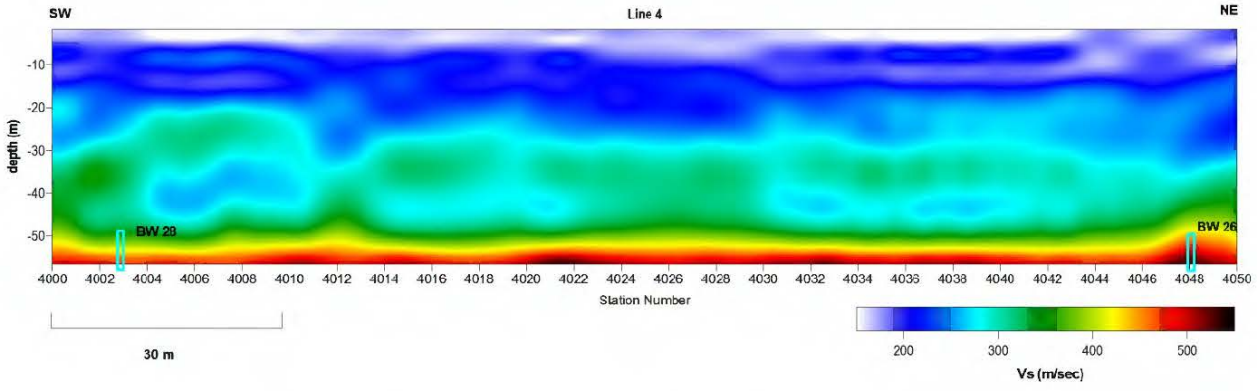

Figure 9. Final shear-wave velocity profile from line 4 of the initial survey. Approximate well locations are indicated at the bottom of the profile.

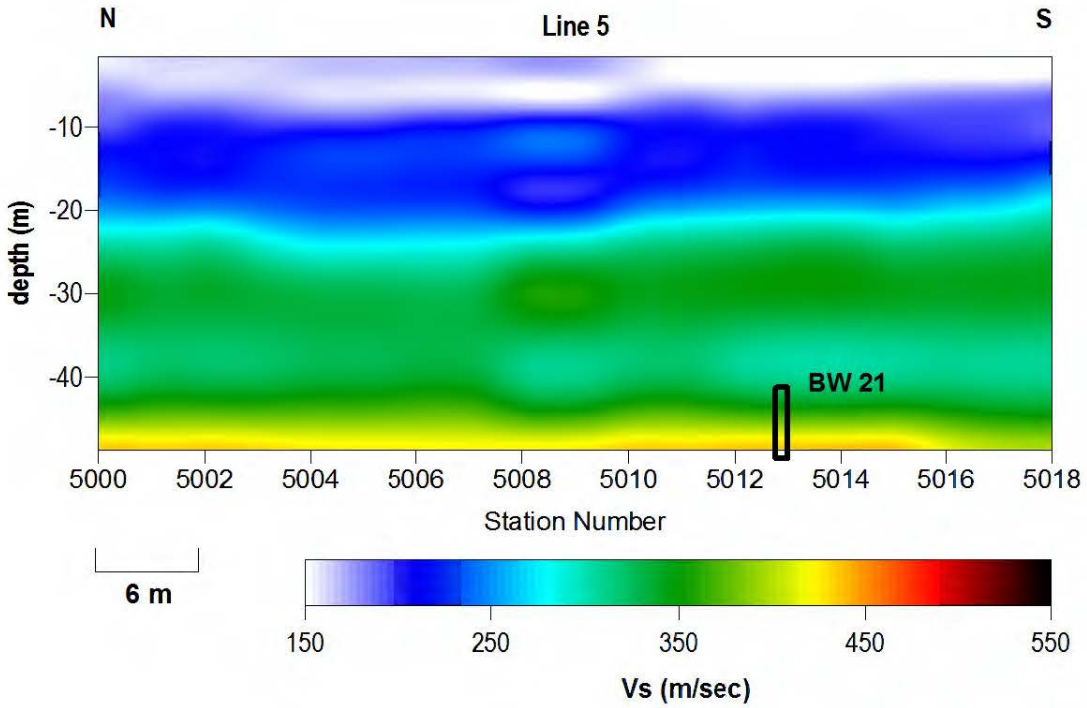

Figure 10. Final shear-wave velocity profile from line 5 of the initial survey. Approximate well location is indicated at the bottom of the profile.

Study II: Follow-up Investigation of Wells 33, 20 and 21, January 2015

Field Layout and Data Acquisition

A follow-up survey was performed on the night of January 22, 2015, to fill in and improve the dataset and enhance the interpretation near wells 33, 20, and 21. Two lines and a 2-D grid of receivers were deployed in the study area (Figure 3). As in the previous survey, seismic receivers were single GeoSpace GS11D 4.5 Hz vertical geophones spaced at 3 m intervals. Line 5 was extended (Table 3) to accommodate the larger processing spread lengths required to enhance resolution of the fundamental mode surface wave on this line. The surface monitoring grid was geospatially located and deployed at the same location as the grid from the initial study. Data were recorded during two nights with a 300+ channel 24-bit Geometrics Geode distributed seismic system. Seismic records were 30 s long with a 2 ms sampling interval. In total, 880 seismic records equivalent to 15.5 GB of data were recorded.

Processing and Analysis

Due to the variations in the characteristics of available energy sources (e.g. distance, speed, length, weight), the signal-to-noise ratio of recorded surface wave energy was less than the initial October 2014 survey for line 1, and greater than the previous survey for line 5. Data were processed consistent with the previous survey. The apparent velocity increase associated with source azimuth was less than 2% for the records that were processed for both lines (Table 4).

Table 3. Number of receivers, total lengths, and wells located within each seismic line acquired in the follow-up investigation.

	# of receivers	line length (m)	well(s)
line 1	48	141	33
line 5	112	331	21, 20

Table 4. Directions of the passive seismic sources and the seismic lines (in degrees counterclockwise from east), the angle of the source with respect to the line (θ), and the percent increase in apparent velocity caused by oblique source orientations (Δv).

	source orientation	line orientation	θ	Δv
line 1	~160	170	~10	1.5%
line 5	80	90	10	1.5%

Results and Interpretation

Dispersion patterns on phase velocity versus frequency plots for line 1 of the follow-up survey have lower signal-to-noise ratio of the fundamental mode Rayleigh wave, and thus greater uncertainty, relative to the initial survey. The general trends observed in the 2-D Vs profile from the follow-up survey (Figure 11) are consistent with observations from the initial survey (Figure 6). The fundamental mode Rayleigh wave energy has higher resolution on phase velocity versus frequency plots obtained in the initial survey, particularly at the northwest end of the line (Figure 12). Therefore, confidence in the bedrock velocities obtained in the initial survey is higher. The shear-wave velocity of bedrock and depth of surface wave penetration are greater on this line relative to other lines at this site, which is suggestive of elevated stress on this line.

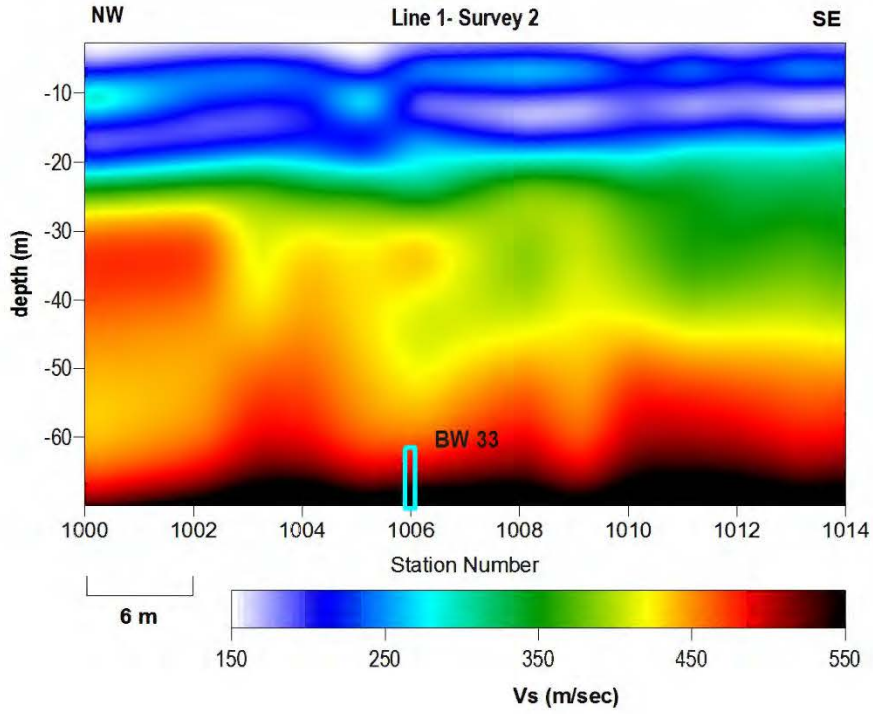

Figure 11. Final shear-wave velocity profile from line 1 of the follow-up survey. Approximate well location is indicated at the bottom of the profile.

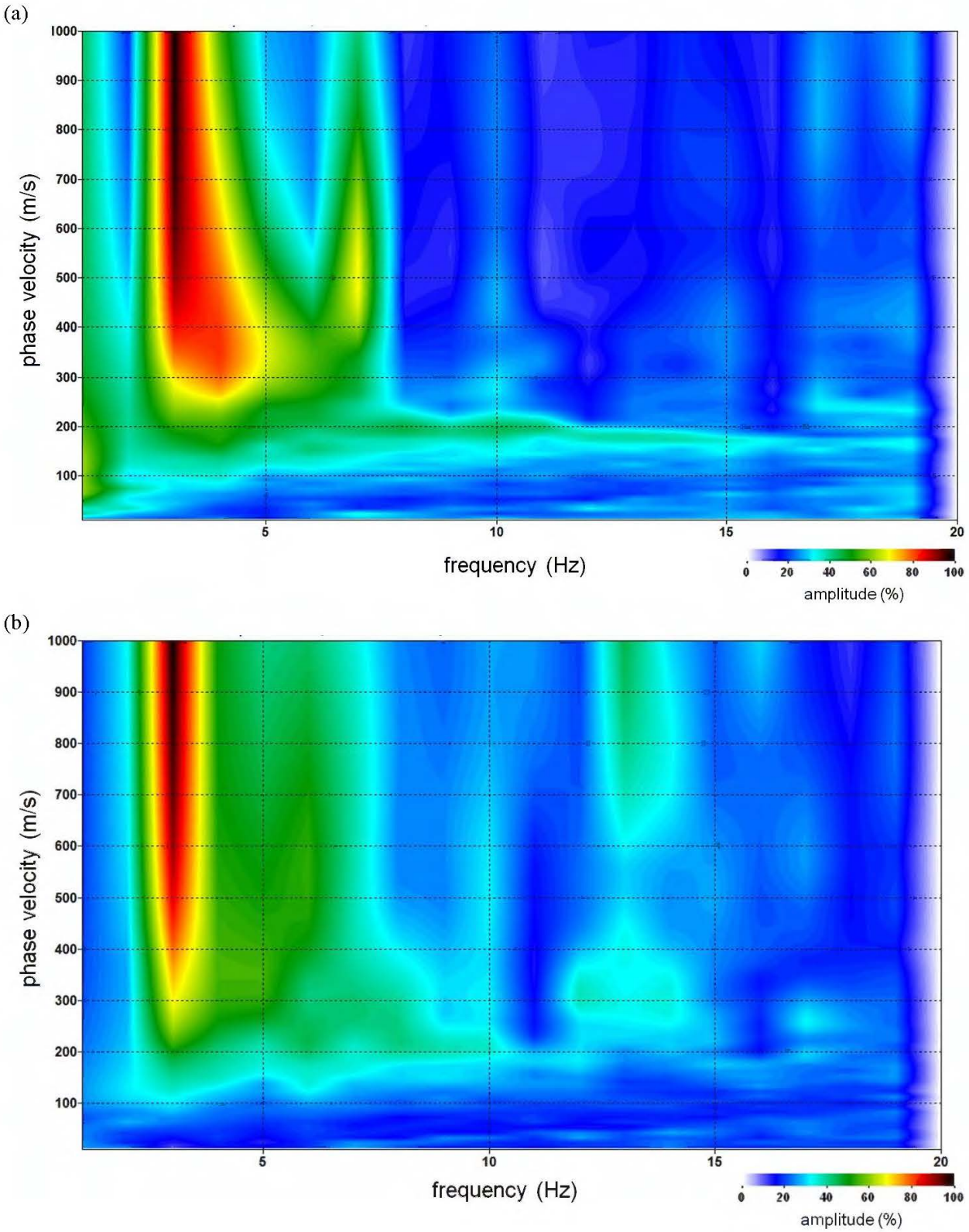

Figure 12. Representative dispersion patterns from line 1 of (a) the initial October 2014 survey and (b) the follow-up January 2015 survey.

The increased length of line 5 allowed for sufficient horizontal sampling to estimate shear-wave velocities both on and off wells 20 and 21. Due to improved signal-to-noise ratio of the fundamental mode Rayleigh wave acquired during this survey, confidence in the 2-D Vs profile (Figure 13) is high. Bedrock velocities are consistent with velocities obtained on other lines at this site. Although there is lateral variability in the bedrock surface that extends from station 5020 to 5050, the absence of any velocity anomalies at depth is indicative of a normal stress regime. The general shape of the bedrock surface is suggestive of a possible channel feature, and its location relative to wells 20 and 21 is most likely coincidental.

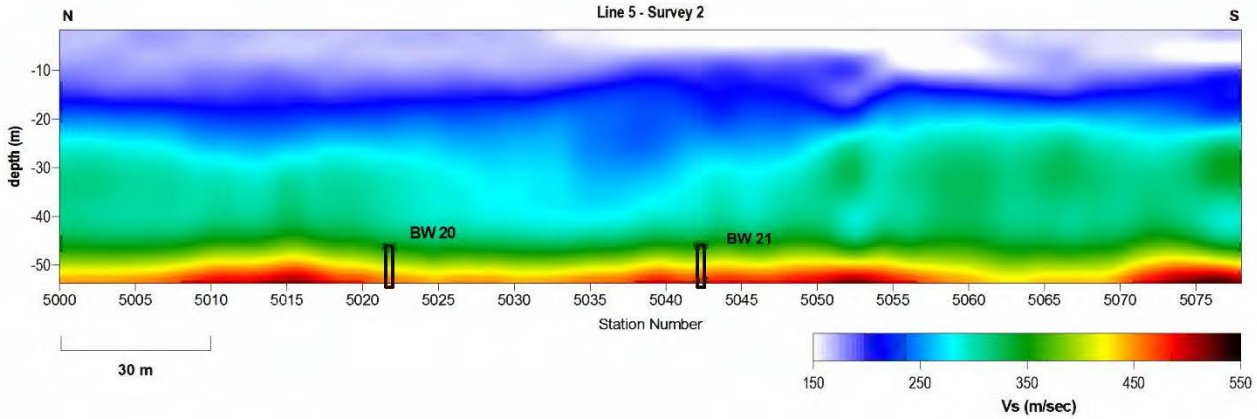

Figure 13. Final shear-wave velocity profile from Line 5 of the January survey. Approximate well locations are indicated at the bottom of the profile.

Comprehensive Interpretation and Discussion

Well 33

A 30% or greater increase is observed in shale bedrock velocity on line 1 in both the initial and follow-up investigation of well 33. Increased bedrock velocity on the southwest end of line 2 near the line 1 intersection (Figure 7) is consistent with this observation. This increased velocity may represent elevated stress due to increased load on an under-supported void roof. A low velocity anomaly beneath this possible tensional dome is not observed at the depths imaged, indicating that the void likely has not migrated above the three-finger dolomite. A priori information from a past sonar survey indicates a relatively small void at this location. While the magnitude of the velocity anomaly is indicative of elevated stress and potential failure, the relatively small volume of this jug will severely limit the amount of collapse breccia from roof rocks that can collect in this relatively small void thereby minimizing any future vertical migration of the void to depths well below ground surface.

Wells 32 and 57

Velocity profiles over these wells suggest a normal stress regime.

Wells 26 and 28

The majority of the profile is representative of a normal stress regime. There is a ~15% increase in bedrock velocity at 50 m depth near well 26. Although this could be indicative of a

localized increase in stress, confidence in this anomaly is relatively low due to low signal-to-noise ratio of the fundamental mode Rayleigh wave.

Wells 20 and 21

Shear-wave velocity of the shale bedrock is representative of a normal stress regime. Although a priori information from a past sonar survey in well 20 indicates a large void, the geometry of the roof may be favorable for evenly distributing stress. This void currently appears to be stable and has a low risk of vertical migration or collapse at the time of this survey. Lateral variability in the bedrock surface above wells 20 and 21 is suggestive of a depositional or erosional feature, such as a paleochannel. Its location relative to wells 20 and 21 is most likely coincidental.

Conclusions

Shear-wave velocities were obtained over seven wells using passive MASW. Rayleigh wave velocities were recorded at frequencies as low as 3 Hz for all lines, achieving depths of investigation ranging from 40 to 60 m or greater. Increased shear velocity over well 33 suggests elevated stress due to increased load on an under-supported roof. While the magnitude of the velocity anomaly suggests vertical migration may be possible, the size of the void estimated during a past sonar survey suggests that any future vertical migration of this relatively small void would most likely be limited to depths well below ground surface. Velocity profiles over wells 20, 21, 26, 28, 32, and 57 likely represent natural geologic variation and a normal stress regime.

References

Dellwig, L.F., 1963, Environment and mechanics of deposition of the Permian Hutchinson Salt Member of the Wellington shale: Symposium on Salt, Northern Ohio Geological Society, p. 74-85.

Dvorkin, J., A. Nur, and C. Chaika, 1996, Stress sensitivity of sandstones: *Geophysics*, v. 61, p. 444-455.

Eberhart-Phillips, D., D.-H. Han, and M.D. Zoback, 1989, Empirical relationships among seismic velocity, effective pressure, porosity, and clay content in sandstone: *Geophysics*, v. 54, p. 82-89.

Holdoway, K.A. 1978, Deposition of evaporites and red beds of the Nippewalla Group, Permian, western Kansas: Kansas Geological Survey Bulletin 215.

Ivanov, J., R.D. Miller, S.L. Peterie, J.T. Schwenk, J.J. Nolan, B. Bennett, B. Wedel, J. Anderson, J. Chandler, and S. Green, 2013, Enhanced Passive Seismic Characterization of High Priority Salt Jugs in Hutchinson, Kansas: preliminary report to Burns & McDonnell Engineering Company.

Khaksar, A., C.M. Griffiths, and C. McCann, 1999, Compressional- and shear-wave velocities as a function of confining stress in dry sandstones: *Geophysical Prospecting*, v. 47, p. 487-508.

Kulstad, R.O., 1959, Thickness and salt percentage of the Hutchinson salt; in, Symposium on Geophysics in Kansas: Kansas Geological Survey Bulletin 137, p. 241-247.

McGuire, D., and B. Miller, 1989, The utility of single-point seismic data: In Geophysics in Kansas, D.W. Steeples, ed.: Kansas Geological Survey Bulletin 226, p. 1-8.

Merriam, D.F., 1963, The Geologic History of Kansas: Kansas Geological Survey Bulletin 162, 317 p.

Merriam, D.F., and C.J. Mann, 1957, Sinkholes and related geologic features in Kansas: Transactions of the Kansas Academy of Science, v. 60, p. 207-243.

Miller, R.D., 2011, Progress report: 3-D passive surface-wave investigation of solution mining voids in Hutchinson, Kansas: Interim report to Burns & McDonnell Engineering Company, January, 9 p.

Miller, R.D., J. Ivanov, S.D. Sloan, S.L. Walters, B. Leitner, A. Rech, B.A. Wedel, A.R. Wedel, J.M. Anderson, O.M. Metheny, and J.C. Schwarzer, 2009, Shear-wave study above Vigindustries, Inc. legacy salt jugs in Hutchinson, Kansas: Kansas Geological Survey Open-file Report 2009-3.

Park, C., R. Miller, D. Laflen, N. Cabrillo, J. Ivanov, B. Bennett, and R. Huggins, 2004, Imaging dispersion curves of passive surface waves [Exp. Abs.]: Annual Meeting of the Soc. of Expl. Geophys., Denver, Colorado, October 10-15, p. 1357-1360.

Sayers, C.M., 2004, Monitoring production-induced stress changes using seismic waves [Exp. Abs.]: Annual Meeting of the Soc. of Expl. Geophys., Denver, Colorado, October 10-15, p. 2287-2290.

Sloan, S.D., S.L. Peterie, J. Ivanov, R.D. Miller, and J.R. McKenna, 2010, Void detection using near-surface seismic methods; *in* Advances in Near-Surface Seismology and Ground-Penetrating Radar, SEG Geophysical Developments Series No. 15, R.D. Miller, J.D. Bradford, and K. Holliger, eds.: Tulsa, Society of Exploration Geophysicists, p. 201-218.

Swineford, A., 1955, Petrography of upper Permian rocks in south-central Kansas: State Geological Survey of Kansas Bulletin 111, 179 p.

Walters, R.F., 1978, Land subsidence in central Kansas related to salt dissolution: Kansas Geological Survey Bulletin 214, 82 p.

Whittemore, D.O., 1990, Geochemical identification of saltwater contamination at the Siefkes subsidence site: Report for the Kansas Corporation Commission.

Whittemore, D.O., 1989, Geochemical characterization of saltwater contamination in the Macksville sink and adjacent aquifer: Kansas Geological Survey Open-file Report 89-35.